



CAN UNCLASSIFIED

DRDC | RDDC  
technologysciencetechnologie



# Inversion of water clouds lidar returns using the azimuthal dependence of the cross-polarization signal

Xiaoying Cao  
Lidar Consultant

Gilles Roy  
DRDC – Valcartier Research Centre

Gregoire Tremblay  
AEREX Avionique Inc.

Optics Letters  
Vol. 43, No. 3 / February 1 2018  
p. 451-454

Date of Publication from Ext Publisher: January 2018

**Defence Research and Development Canada**  
**External Literature (P)**  
DRDC-RDDC-2018-P058  
May 2018

CAN UNCLASSIFIED

**IMPORTANT INFORMATIVE STATEMENTS**

This document was reviewed for Controlled Goods by Defence Research and Development Canada (DRDC) using the Schedule to the *Defence Production Act*.

Disclaimer: This document is not published by the Editorial Office of Defence Research and Development Canada, an agency of the Department of National Defence of Canada but is to be catalogued in the Canadian Defence Information System (CANDIS), the national repository for Defence S&T documents. Her Majesty the Queen in Right of Canada (Department of National Defence) makes no representations or warranties, expressed or implied, of any kind whatsoever, and assumes no liability for the accuracy, reliability, completeness, currency or usefulness of any information, product, process or material included in this document. Nothing in this document should be interpreted as an endorsement for the specific use of any tool, technique or process examined in it. Any reliance on, or use of, any information, product, process or material included in this document is at the sole risk of the person so using it or relying on it. Canada does not assume any liability in respect of any damages or losses arising out of or in connection with the use of, or reliance on, any information, product, process or material included in this document.

# Inversion of water clouds lidar returns using the azimuthal dependence of the cross-polarization signal

Xiaoying Cao<sup>1</sup>, Gilles Roy<sup>2,\*</sup> and Gregoire Tremblay<sup>3</sup>

<sup>1</sup>Lidar consultant, Nepean, Ontario, Canada

<sup>2</sup>Defence Research Development Canada Valcartier, Québec, Canada

<sup>3</sup>AEREX avionic, Québec, Canada

\*Corresponding author: [gilles.roy@drdc-rddc.gc.ca](mailto:gilles.roy@drdc-rddc.gc.ca)

Received Month X, XXXX; revised Month X, XXXX; accepted Month X, XXXX; posted Month X, XXXX (Doc. ID XXXXX); published Month X, XXXX

The contrast in the azimuthal pattern of cross polarized lidar data is used directly to retrieve the extinction coefficient profile of water droplet clouds. Using Monte Carlo simulation, we demonstrate that there is a simple mathematical relationship between the optical depth and the contrast of the cross polarization azimuthal pattern. This relation is independent of the water cloud droplets size, cloud position and extinction profile. Derivation of the extinction profile of a water droplets cloud is obtained directly using the simple mathematical relationship without performing lidar equation inversion. The technique is limited to spherical particles.

OCIS Codes: (010.3640) lidar, (290.4210) Multiple scattering, (290.5855) Scattering, polarization.

Retrieval of extinction coefficient of dense water clouds is problematic because stable lidar inversion techniques (Klett and Weimann, [1] and [2]) require an estimate of the extinction or optical depth value at the back end of the cloud. Using Hu [3] relationship between integrated single scattering fraction and accumulated linear depolarization ratio for water droplets, a LAD (Layer Accumulated Depolarization) inversion technique has been developed [4]. The LAD inversion technique is interesting but remains sensitive to the accurate determination of a constant specific to the lidar.

Carswell and Pal<sup>5</sup> reported, in 1980, observations of polarization patterns in multiply-scattered returns from controlled-environment clouds. They repeated these observations in atmospheric clouds in 1985<sup>6</sup>. Rakovic and Kattawar<sup>7</sup> provided, in 1998, a consistent theoretical analysis of these findings: a simple model of second-order scattering from spherical particles reproduces quite well the observed patterns. Roy et al. [8] suggested multiply scattered lidar returns contain retrievable information on cloud parameters, e.g. optical depth (OD) and droplet size, that has not yet been exploited.

In this paper, we analyze the secondary polarization azimuthal pattern generated by Monte Carlo simulation and show that the contrast of azimuthal pattern is practically independent of the water cloud range and droplet size. A relationship is established between the contrast of the symmetrical azimuthal pattern and the optical depth. That relationship is used to retrieve the extinction profile of the water clouds. In order to better understand the mechanism of polarized multiple scattering, Monte Carlo (MC) simulation has been performed. The Unique MC simulator is a multithreaded software based on the Bohren and Huffman Mie scattering algorithm. The simulator reproduces the characteristics of a Flash Lidar system. It consists of an emitter/receiver system, a target and a

propagation range including aerosols of various properties. The particularity of the Unique MC is its capability to image the scattered light on a detector array [9]. In here, the imaging system is  $256 \times 256$  pixels and covers an FOV of  $16 \text{ mrad} \times 16 \text{ mrad}$ . The output of the MC can be transformed in  $\text{W/m}^2/\text{J}$ . Fig. 1 illustrates the measurement concept emulated by MC. Fig. 2 shows the azimuthal pattern obtained for a simulation of a penetration through a cloud depth of 50 m with constant extinction of  $0.03 \text{ m}^{-1}$  starting at 1000 m. The image at the top contains all the scattering orders, while the image at the bottom contains the second scattering order only. The second order scattering cross polarization follows a  $\cos(4\phi)$  pattern; it means that there is no second-order scattered energy for azimuths equal to  $0^\circ$ ,  $90^\circ$ ,  $180^\circ$ ,  $270^\circ$ . In multiple scattering conditions (top part of Fig. 2) there is clearly a fair amount of energy at those angles.

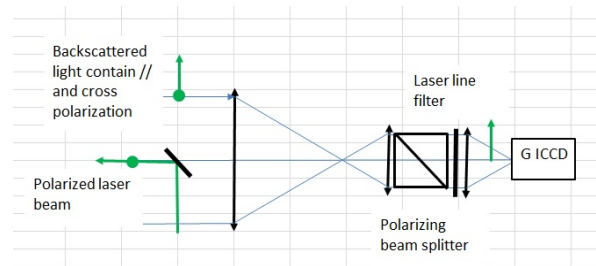


Fig. 1. Lidar set up to capture the azimuthal secondary polarization. The linearly polarized source is emitted on axis (lower left). The received signal is collimated through a polarizer and the secondary polarization is imaged on the camera (right).

The images are divided into 32 concentric FOV rings with  $0.5 \text{ mrad}$  increment from one ring to the next. Each ring is divided into 5-degrees segments in azimuth. The

energy contained in each of these segments is calculated and then used as input data for the best fit for a given ring. The contrast is calculated by doing a best fit to the equation,  $I = a_i \cos(4\phi) + b_i$ , where  $a_i$  and  $b_i$  are the fit parameters for each MC data set ( $a_i < 0$  and  $b_i > 0$ ).

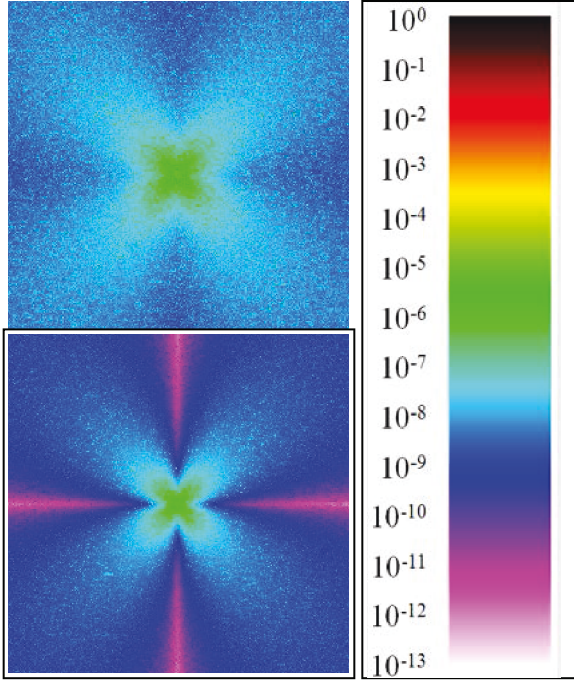


Fig. 2. Secondary polarization azimuth patterns from returns of all scattering orders (top) and 2nd scattering order only (bottom).

The contrast is defined as:  $(I_{\max} - I_{\min}) / (I_{\max} + I_{\min})$  and is therefore equal to

$$C(\theta_i) = \frac{-a_i}{b_i}, \quad (1)$$

where  $\theta_i$  is the FOV angle. The dependence of the contrast on optical depth has been assessed by producing new MC simulations for each increment of 5 meters of penetration in the clouds.

A total of 6 MCs has been performed. The wavelength is 532 nm and the water cloud droplets distribution were represented by two gamma distributions ( $a=4$  and  $b=0.5$  for effective radius of 11.9 microns, and  $a=7$  and  $b=1.5$  for effective radius of 5.95  $\mu\text{m}$ ). The effective radius is defined as  $\langle r^3 \rangle / \langle r^2 \rangle$ . Fig. 3 shows the contrast as a function of optical depth for cloud #4 of table 1. The contrast,  $C(\theta_i)$  is calculated over an angular width of 1 mrad for FOV,  $\theta_i$ , at 2, 4, 8, and 12 mrad. The collecting optics was set to 0.2 m in diameter with a focal length of 0.76 m. The object plane of the imaging system is set at 575 m (for an optical depth of 2.25). At that distance, the image on the camera is at the focus of the telescope and the contrasts obtained at the different FOVs superpose well. Figure 3 allows

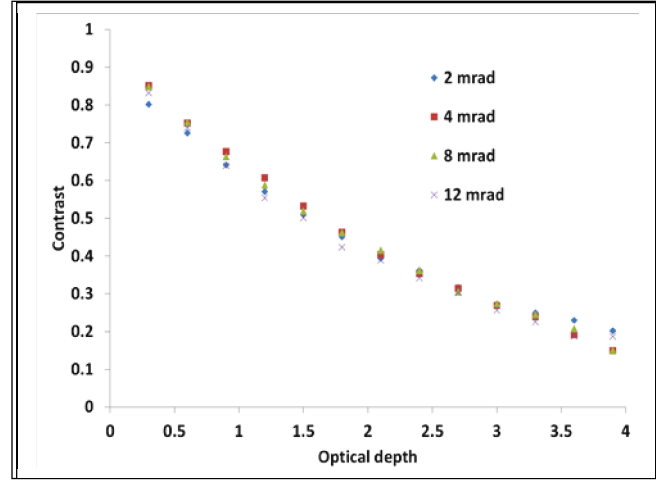


Fig. 3. Contrast as a function of optical depth for cloud #4 of table 1. The contrast is calculated over an angular width of 0.5 mrad centered on 2, 4, 8, 12 mrad. The object plane of the imaging system is set at 575 m (for an optical depth of 2.25).

**Table 1 Clouds position and cloud profiles used for the MC. Each cloud has maximum optical depth of 4.5.**

	$r$ ( $\mu\text{m}$ )	Cloud position (m)	Cloud Profile
#1	11.9	500 -650	Triangular
#2	5.95	500 -650	Triangular
#3	11.9	500 -650	Flat
#4	5.95	500 -650	Flat
#5	5.95	100-120	Triangular
#6	5.95	100-120	Flat

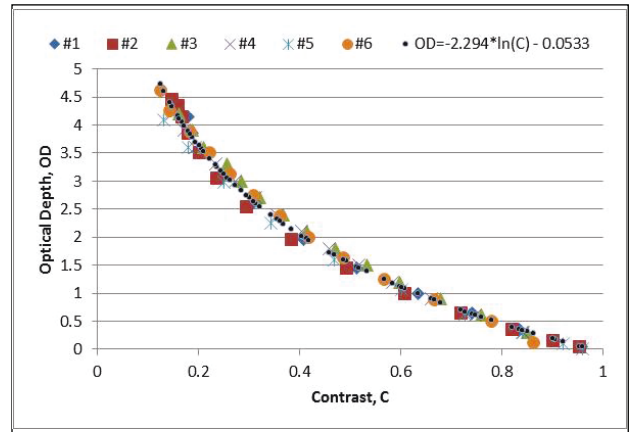


Fig. 4. Variation of the optical depth as a function of the contrast for the various clouds defined in table 1. Different plotting symbols are used for different droplet sizes, clouds position and extinction profile.

seeing that, even for ODs different from 2.25, thus for distances away from the object plane, the contrast values  $C(\theta_i)$  do not show much variability with respect to FOV and the average value from 3 to 12 mrad is used in the calculations that follow. Smaller FOVs contrast values are very close to the laser beam and are affected by the laser beam foot print.

The variation of the optical depth as a function of the contrast for the various clouds defined in table 1 is shown in Fig. 4. Different plotting symbols are used for different droplet sizes, clouds position and extinction coefficient profile. The best fit relationship of the optical depth as a function of the contrast is given by

$$\tau(C) = -2.294 \ln(C) - 0.0533 . \quad (2)$$

The relationship between the optical depth and the contrast remarkably appears to be independent of the cloud position, extinction profile, and water droplet size. Since the optical depth is defined as  $\tau = \int_0^z \sigma(z) dz$ , and as the optical depth of a cloud can be written as:  $\tau(C(z))$  the extinction profile can be obtained from

$$\sigma(z) = \frac{d\tau(C)}{dC} \cdot \frac{dC(z)}{dz} . \quad (3)$$

Wherein, using eq. 2,

$$\frac{d\tau(C)}{dC} = \frac{-2.294}{C} , \quad (4)$$

and  $\frac{dC(z)}{dz}$  is derived from the measured contrast as a function of penetration depth in the cloud.

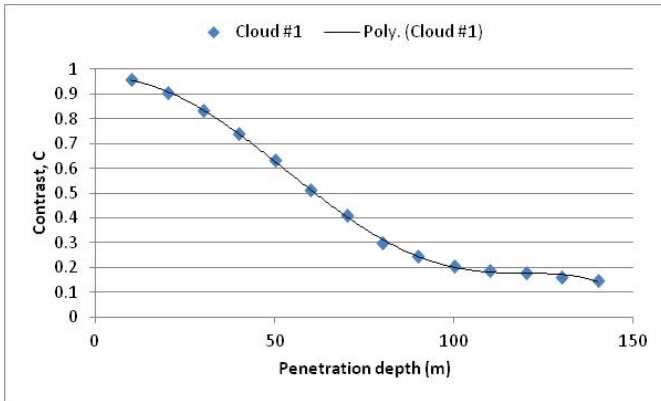


Fig. 5. Contrast,  $C$  as a function of penetration depth for water clouds #1 of table 1. The plain black curve is a 5<sup>th</sup> order polynomial fit

In order to validate the concept of extinction coefficient retrieval, Eq. 3 and 4 were first applied to triangular cloud profiles 1 and 2 of table 1. First, the variation of contrast as a function of optical depth is calculated, plot, and then a polynomial fit is used to provide an analytical expression to  $C(z)$  and to  $dC(z)/dz$ . Fig. 5, show  $C(z)$  and its polynomial fit for cloud #1, and the result for the retrieved extinction for cloud #1 and #2 are displayed in Fig. 6. The second validation test (Fig. 7) is performed using cloud parameters completely outside the set of parameters used to derive eq. 1: 1) the cloud base is set at a range of 1000m, 2) the water droplets have an effective radius of 3.32  $\mu\text{m}$  (obtained with a gamma distribution with  $a=3$ ,  $b=1.5$ ), 3), the cloud extinction profile increases linearly for the first 50 m and has a constant extinction for the next 50 m. For optical depth smaller than 3, the recovered extinction coefficient is reasonably close to the true extinction profile.

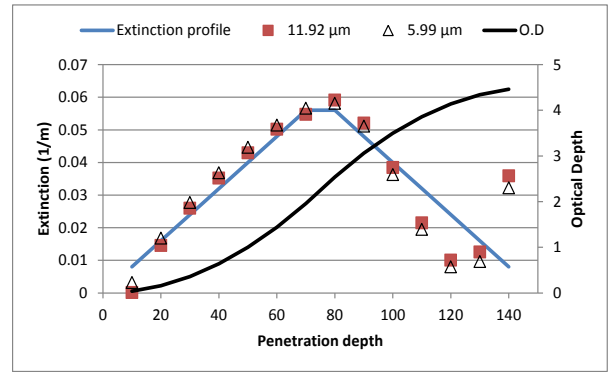


Fig. 6. Extinction coefficient recovery using Eq. 2 and 3 for water clouds #1 and #2 of table 1.

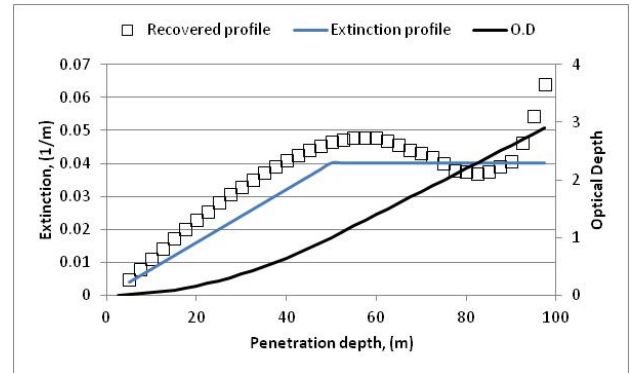


Fig. 7. Extinction coefficient recovery using Eq. 2 and 3 for a water cloud base at 1000m and with an effective radius of 3.32  $\mu\text{m}$

The technique uses a best fit of a relationship between the optical depth and the contrast. Although the  $R^2$  is better than 0.99, there is intrinsic small variability due to the cloud profiles and droplets size. This small variability persists independently of the number of photons used to perform the MC and increase with the optical depth. The fact that the

technique use the product of derivatives (see Eq. 3) to retrieve the extinction profile, make it more sensitive to errors. Therefore theoretically, an optical depth of 3 appears to be the maximum value the technique could be applied to.

The technique is based on contrast blur caused by multiple scattering. The capability of a real system to recover the true extinction profile will be affected by the quality of the imaging system. So blur caused by too large out-of-focus error will induce important malfunction of the proposed algorithm.

Fig. 8 compares the images obtained for a measurement at an optical depth of 1 with perfect focus at a range of 1050m with measurement performed at the exact same range but focus set at a range of 100m.

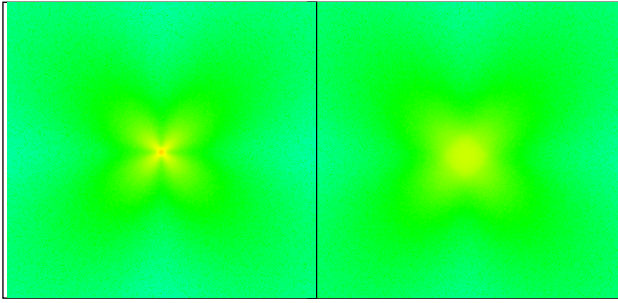


Fig. 8. Comparison of the images obtained for a measurement at an optical depth of 1 at a range of 1050m with perfect focus (left) with measurement performed at the same range with focus set at a range of 100m (right).

Visual inspection of the out-of-focus image gives a good idea that images obtained with significant defocus will not be usable. A contrast analysis (Fig. 9) clearly indicates that the proposed technique cannot be used for significantly out-of-focus images. The data presented in Fig. 3 has shown to within a certain distance from the focused object plane, the method does function. The extent of that region could be technically related to the depth of focus of the optical system. This blurring cause by out of focus imaging most likely explain the lower contrast reported in reference 8 where the measurement were performed using an aerosols chamber at close range (100m). Measurements performed on real cloud (see [10]) at a range of 1400m have shown a  $d\tau(C)/dC = -2.41/C$  which is very close to the model value of Eq. 4. Optics with large f-number can certainly be used to overcome focus adjustment.

Finally, it is not necessary to use a G-ICCD camera to perform contrast measurements. Pal and Carswell have suggested the use of masks. The measurement could also be done using, with some adjustment, the multiple-scattering polarization lidar developed under the leadership of Okamoto [11].

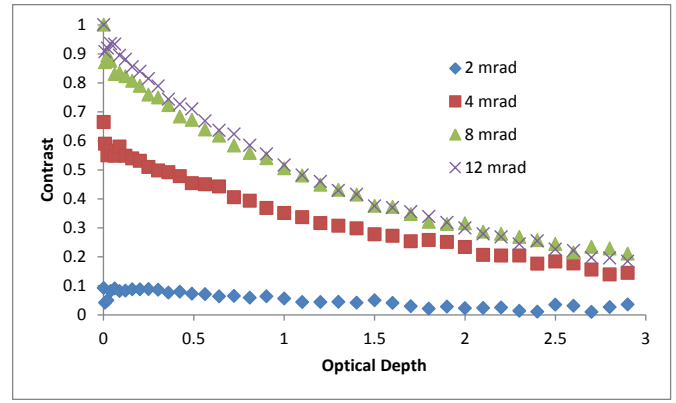


Fig. 9. Contrast as a function of optical depth for a cloud base at 1000m and extinction profile shown in Fig. 6. The contrast is calculated over an angular width of 0.5 mrad at 2, 4, 8, 12 mrad. The object plane of the imaging system is set at 100 m.

## References

1. J. D. Klett, Appl. Opt. 20, 211–220 (1981).
2. J. A. Weinman, Appl. Opt. 27, 3994–4001 (1988).
3. Y. Hu, et al., Opt. Lett. 31, 1809–1811 (2006).
4. G. Roy, X. Cao, Appl. Opt. 49, 1630 - 1635, (2010)
5. A.I. Carswell and S.R. Pal, Appl. Opt. 19, 4123-4126 (1980)
6. S.R. Pal and A.I. Carswell, Appl. Opt. 24, 3464-3471 (1985)
7. Milun J. Rakovic, George W. Kattawar, Appl. Opt. 37, 3333-3338 (1998)
8. N. Roy, G. Roy, L. R. Bissonnette and J-R. Simard, Appl. Opt. 43, 2777-2785, (2004)
9. G. Tremblay, G. Roy, 27rd International Laser Radar Conference, New York, USA, (2015)
10. G. Roy, N. Roy and L. R. Bissonnette, 22 rd International Laser Radar Conference, Matera, Italia, (2004)
11. H. Okamoto, K. Sato, T. Nishizawa, N. Sugimoto, T. Makino, Y. Jin, A. Shimizu, T. Takano and M. Fujikawa, Opt. Express 25, 30054-30067 (2016)

## References full citation listings.

1. J. D. Klett, "Stable analytical inversion solution for processing lidar returns," Appl. Opt. 20, 211–220 (1981).
2. J. A. Weinman, "Derivation of atmospheric extinction profiles and wind speed over the ocean from a satellite-borne lidar," Appl. Opt. 27, 3994–4001 (1988).
3. Y. Hu, et al., "Simple relation between lidar multiple scattering and depolarization for water clouds," Opt. Lett. 31, 1809–1811 (2006).
4. G. Roy, X. Cao, "Inversion of water cloud lidar signals based on accumulated depolarization ratio," Appl. Opt. 49, 1630 - 1635, (2010)
5. A.I. Carswell and S.R. Pal, "Polarization anisotropy in lidar multiple scattering from clouds," Appl. Opt. 19, 4123-4126 (1980)
6. S.R. Pal and A.I. Carswell, "Polarization anisotropy in lidar multiple scattering from atmospheric clouds," Appl. Opt. 24, 3464-3471 (1985)
7. Milun J. Rakovic, George W. Kattawar, "Theoretical analysis of polarization patterns from incoherent backscattering of light," Appl. Opt. 37, 3333-3338 (1998)
8. N. Roy, G. Roy, L. R. Bissonnette and J-R. Simard, "Measurement of the azimuthal dependence of cross-polarized lidar returns and its relation to optical depth," Appl. Opt. 43, 2777-2785, (2004)
9. G. Tremblay, G. Roy, "High fidelity imaging algorithm for the Unique Monte Carlo simulator," 27th International Laser Radar Conference, New York, USA, (2015)
10. G. Roy, N. Roy and L. R. Bissonnette, "Measurement of multiple scattering in cloud using a gated intensified CCD camera," 22nd International Laser Radar Conference, Matera, Italia, (2004)
11. H. Okamoto, K. Sato, T. Nishizawa, N. Sugimoto, T. Makino, Y. Jin, A. Shimizu, T. Takano and M. Fujikawa, "Development of a multiple-field-of-view multiple-scattering polarization lidar: comparison with cloud radar", Opt. Express 25, 30054-30067 (2016)

DOCUMENT CONTROL DATA		
*Security markings for the title, authors, abstract and keywords must be entered when the document is sensitive		
1. ORIGINATOR (Name and address of the organization preparing the document. A DRDC Centre sponsoring a contractor's report, or tasking agency, is entered in Section 8.)  <b>OSA—The Optical Society 2010 Massachusetts Ave., N.W. Washington, D.C. 20036-1012 USA</b>		2a. SECURITY MARKING (Overall security marking of the document including special supplemental markings if applicable.)  <b>CAN UNCLASSIFIED</b>
		2b. CONTROLLED GOODS  <b>NON-CONTROLLED GOODS DMC A</b>
3. TITLE (The document title and sub-title as indicated on the title page.)  <b>Inversion of water clouds lidar returns using the azimuthal dependence of the cross-polarization signal</b>		
4. AUTHORS (Last name, followed by initials – ranks, titles, etc., not to be used)  <b>Cao, X.; Roy, G.; Tremblay, G.</b>		
5. DATE OF PUBLICATION (Month and year of publication of document.)  <b>January 2018</b>	6a. NO. OF PAGES (Total pages, including Annexes, excluding DCD, covering and verso pages.)  <b>5</b>	6b. NO. OF REFS (Total references cited.)  <b>11</b>
7. DOCUMENT CATEGORY (e.g., Scientific Report, Contract Report, Scientific Letter.)  <b>External Literature (P)</b>		
8. SPONSORING CENTRE (The name and address of the department project office or laboratory sponsoring the research and development.)  <b>DRDC - Valcartier Research Centre Defence Research and Development Canada 2459 route de la Bravoure Quebec (Quebec) G3J 1X5 Canada</b>		
9a. PROJECT OR GRANT NO. (If appropriate, the applicable research and development project or grant number under which the document was written. Please specify whether project or grant.)	9b. CONTRACT NO. (If appropriate, the applicable number under which the document was written.)	
10a. DRDC PUBLICATION NUMBER (The official document number by which the document is identified by the originating activity. This number must be unique to this document.)  <b>DRDC-RDDC-2018-P058</b>	10b. OTHER DOCUMENT NO(s). (Any other numbers which may be assigned this document either by the originator or by the sponsor.)	
11a. FUTURE DISTRIBUTION WITHIN CANADA (Approval for further dissemination of the document. Security classification must also be considered.)  <b>Public release</b>		
11b. FUTURE DISTRIBUTION OUTSIDE CANADA (Approval for further dissemination of the document. Security classification must also be considered.)		

12. KEYWORDS, DESCRIPTORS or IDENTIFIERS (Use semi-colon as a delimiter.)

Lidar; Extinction coefficient retrieval; Multiple scattering; Scattering, polarization

13. ABSTRACT/RÉSUMÉ (When available in the document, the French version of the abstract must be included here.)

The contrast in the azimuthal pattern of cross polarized lidar data is used directly to retrieve the extinction coefficient profile of water droplet clouds. Using Monte Carlo simulation, we demonstrate that there is a simple mathematical relationship between the optical depth and the contrast of the cross polarization azimuthal pattern. This relation is independent of the water cloud droplets size, cloud position and extinction profile. Derivation of the extinction profile of a water droplets cloud is obtained directly using the simple mathematical relationship without performing lidar equation inversion. The technique is limited to spherical particles.